

Modulation response of nanolasers: What rate equation approaches miss

Roland Aust¹ (roland.aust@physik.tu-berlin.de), Thorben Kaul¹, Benjamin Lingnau¹, and Kathy Lüdge²
 1: Technische Universität Berlin, Institut für Theoretische Physik, Germany
 2: Freie Universität Berlin, Fachbereich Physik, Germany

Abstract—Rate equation approaches are a standard method to describe and examine the dynamics of various semiconductor lasers, including nanolasers with high spontaneous emission rates. Using the more complex Bloch equation model we investigate the impact of the internal timescales on the modulation response and demonstrate the limitation of rate equation approaches for systems where photon decay rate and polarization decay have similar orders of magnitude.

I. INTRODUCTION

Decreasing the cavity volume of nanostructured semiconductor lasers entails a variety of consequences on the emission properties of the device, especially due to the increased rate of spontaneous emission [2]. Previous works on nanolaser devices already discussed how the Purcell-enhanced spontaneous emission may increase the modulation bandwidth below threshold [3] or reduce it above threshold [4]. However, extensive microscopic modeling of the light emitting characteristics of nanolasers showed that care has to be taken, as rate equation results may underestimate the modulation properties [5] and also may misinterpret the impact of the microscopic scattering processes [6], [7]. In the present paper we want to deepen the understanding of the interplay between the different timescales that are present in such a nanolaser device, especially investigating the effect of photon lifetime, polarization decay and spontaneous emission rate. Thus, by using a simplified microscopically-adapted Bloch-equation model, we analyze the impact of varying timescales on the dynamic response of the laser and discuss what rate equations miss for the case of similar photon and polarization decay. We also show that it is hard to predict the effect of spontaneous emission enhancement without exactly knowing the remaining timescales, as both, a better and a decreased

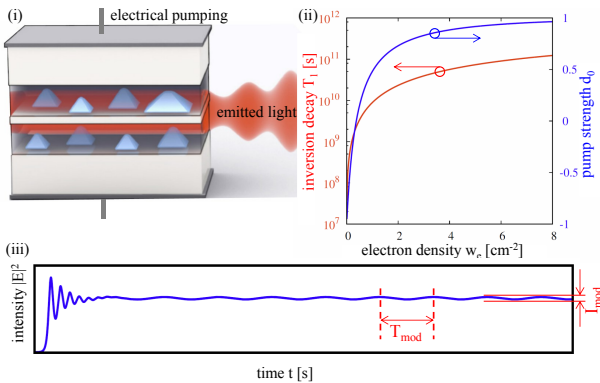


Fig. 1. (i) Quantum dot laser scheme [1]; (ii) Inversion decay $T_1^{-1}(w_e)$ (red line) and pump strength $d_0(w_e)$ (blue line) in dependence of the wetting layer electron density w_e ; (iii) Time series with modulated pump current (modulation period T_{mod}) and resulting modulation amplitude I_{mod} .

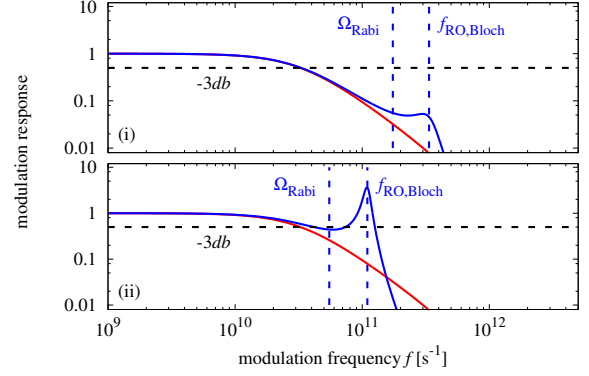


Fig. 2. Modulation response versus the modulation frequency f_{mod} for rate (red lines) and Bloch (blue lines) equations. The corresponding Rabi Ω_{Rabi} and relaxation oscillation frequencies of the Bloch system $f_{RO,Bloch}$ are marked by vertical blue dashed lines. Parameters: $\kappa = 10^{11} s^{-1}$, $\tau_{sp}^{-1} = 10^{10} s^{-1}$, $w_e = 6 \cdot 10^{11} cm^{-2}$; (i) $\gamma = 10^{12} s^{-1}$, (ii) $\gamma = 10^{11} s^{-1}$.

modulation bandwidth can result.

II. MODELING

We describe our quantum-dot nanolaser system by using the following Bloch equation model containing equations for the field amplitude E , the polarization p , and the inversion d . It is adapted from simple laser equations [8] with additional Purcell-enhanced spontaneous emission rate [3] and microscopic details of quantum-dot laser dynamics [1], [9].

$$\dot{E} = -\kappa E + 2Z^{QD}\Gamma|g|p + \frac{Z^{QD}\Gamma\beta F_P}{\tau_{sp}E} \left(\frac{d+1}{2}\right)^2 \quad (1)$$

$$\dot{p} = -\gamma p + |g|Ed \quad (2)$$

$$\dot{d} = -4|g|Ep + \frac{d_0(w_e) - d}{T_1(w_e)} - \frac{F_P}{\tau_{sp}} \left(\frac{d+1}{2}\right)^2 \quad (3)$$

The dominating timescales are the polarization decay γ , the photon decay rate κ and the rate of spontaneous emission τ_{sp} . The Purcell and spontaneous emission factors are indicated with F_P and β , respectively, Z^{QD} denotes the number of quantum dots in the active region, and g is the gain. For simplicity we assume equal electron and hole carrier densities $\rho_e = \rho_h$ in the quantum dots and define the inversion as $d = \rho_e - \rho_h - 1$. The carrier-carrier coulomb scattering processes needed to fill the confined quantum-dot levels are modeled by the inversion lifetime $T_1(w_e) = (S^{in} + S^{out})^{-1} \cdot 10^{-12}$ and the pump strength $d_0(w_e) = \frac{2S^{in}}{S^{in} + S^{out}} - 1$, where the scattering rates S^{in}, S^{out} are described in [1], [9]. In this simplified approach the carrier density in the surrounding quantum-well

$w_{e/h}$ takes the role of the pump current. Figure 1(ii) depicts the dependence of T_1 and d_0 on the quantum-well carrier density. For increasing occupation in the well, both quantities increase.

Eliminating the polarization dynamics of Eq. (2) adiabatically ($\dot{p} = 0$) [8] and using the resulting static relation $p(E, d)$ within the two remaining equations leads us to the corresponding rate equation system. For the case of fast polarization decay γ the expected results of both models are equal, however we discuss the deviations for the case of $\kappa \approx \gamma$ and the resulting consequences for the impact of τ_{sp} on the modulation response.

III. RESULTS

Figure 2 shows the small signal modulation dynamics of the laser using both modeling approaches. The deviation between the rate and the Bloch equation approach is obvious and can be explained with the resonance induced by the Rabi-oscillations (Ω_{Rabi}). For the Bloch system, both sub-figures show a (local) maximum of the response, whereas the rate equation system is strictly monotonically decreasing. For Fig. 2(i) $\gamma > \kappa$ holds, which leads to a resonance noticeably larger than the cutoff frequency f_{-3db} and thus the cutoff frequencies of the rate equation approach do not differ from the Bloch equation system. When the polarization decay γ approaches the photon decay κ (see Fig. 2(ii)) the modulability of the Bloch system is noticeable improved by the additional resonance. However, with the chosen set of parameters, the response drops below the threshold of -3db, before increasing again and forming the typical resonance peak at $f_{RO,Bloch}$. This cannot be modeled by the rate equation system due to its missing polarization dynamics. Hence, we restrict our investigations in the following to the Bloch equation system. Figure 3 shows the modulation response curves of the Bloch system in dependence of the spontaneous emission rate τ_{sp}^{-1} . Additionally, the eigenvalues of the linearized system are plotted. Their imaginary parts $\Im(\lambda_i)$ are marked by filled circles, color coded by the value of the largest real part $\Re(\lambda_i)$. In both sub-figures we recognize an increasing largest real part $\Re(\lambda_i)$ for higher spontaneous emission rates, which obviously weakens the resonance peaks. Fig. 3(i) shows situations similar to Fig. 2(ii) ($\gamma \approx \kappa$). By adjusting the values of the time scales γ and κ (see Fig. 3(ii)), we may omit the early drop below the threshold of -3db. Then, with increasing spontaneous emission rate, the cutoff frequency is increased, which broadens the modulation bandwidth of the nanolaser device.

IV. CONCLUSION

We investigate the effect of large variations in the spontaneous emission rate of a nanolaser on the modulation response. We show that depending on the internal timescales, especially on the frequency and damping of the Rabi-oscillations, either an increase or a decrease of the bandwidth can be expected. Further we show that rate equation models that are widely used to describe the modulation response of lasers may lead to wrong predictions for the case of nanolasers with equal polarization and photon decay rates.

ACKNOWLEDGMENT

This work is supported by Deutsche Forschungsgemeinschaft in the framework of SFB 787, project B2.

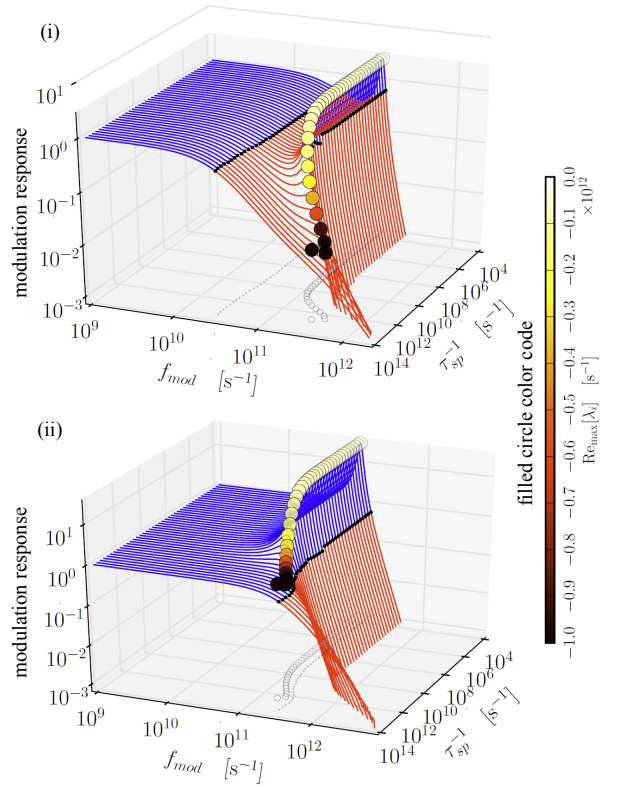


Fig. 3. Modulation response vs. f_{mod} vs. different spontaneous emission rates τ_{sp}^{-1} (Bloch equations). Blue regions represent the imaginary parts above, red regions below f_{-3db} . Filled circles indicate the imaginary parts of the eigenvalues, color coded by the value of the real part. White circles and gray dots on the $\tau_{sp}^{-1} - f_{mod}$ -base plane are the projections of the imaginary part circles and the cutoff frequency dots. Parameters: $w_e = 8 \cdot 10^{11} \text{ cm}^{-2}$; (i) $\kappa = 10^{11} \text{ s}^{-1}$, $\gamma = 10^{11} \text{ s}^{-1}$, (ii) $\kappa = 10^{12} \text{ s}^{-1}$, $\gamma = 10^{12} \text{ s}^{-1}$.

REFERENCES

- [1] K. Lüdge, B. Lingnau, C. Otto, and E. Schöll, "Understanding electrical and optical modulation properties of semiconductor quantum-dot lasers in terms of their turn-on dynamics," *Nonlinear Phenom. Complex Syst.*, vol. 15, no. 4, pp. 350–359, 2012.
- [2] D. B. Li and C. Z. Ning, "Interplay of various loss mechanisms and ultimate size limit of a surface plasmon polariton semiconductor nanolaser," *Opt. Express*, vol. 20, no. 15, p. 1648, 2012.
- [3] E. K. Lau, A. A. Lakhani, R. S. Tucker, and M. C. Wu, "Enhanced modulation bandwidth of nanocavity light emitting devices," *Opt. Express*, vol. 17, no. 10, pp. 7790–7799, 2009.
- [4] K. A. Shore, "Modulation bandwidth of metal-clad semiconductor nanolasers with cavity-enhanced spontaneous emission," *Electron. Lett.*, vol. 46, no. 25, pp. 1688–1689, 2010.
- [5] M. Lorke, T. Suhr, N. Gregersen, and J. Mørk, "Theory of nanolaser devices: Rate equation analysis versus microscopic theory," *Phys. Rev. B*, vol. 87, p. 205310, 2013.
- [6] M. Lorke, T. R. Nielsen, and J. Mørk, "Influence of carrier dynamics on the modulation bandwidth of quantum-dot based nanocavity devices," *Appl. Phys. Lett.*, vol. 97, p. 211106, 2010.
- [7] T. Suhr, N. Gregersen, K. Yvind, and J. Mørk, "Modulation response of nanolasers and nanolasers exploiting purcell enhanced spontaneous emission," *Opt. Express*, vol. 18, no. 11, pp. 11 230–11 241, 2010.
- [8] C. Z. Ning and H. Haken, "Elimination of variables in simple laser equations," *Appl. Phys. B*, vol. 55, no. 2, pp. 117–120, 1992.
- [9] K. Lüdge, "Modeling quantum dot based laser devices," in *Nonlinear Laser Dynamics - From Quantum Dots to Cryptography*, K. Lüdge, Ed. Weinheim: WILEY-VCH Weinheim, 2012, ch. 1, pp. 3–34.